

Robust Stability Analysis of Bilateral Teleoperation Systems Using Admittance-Type Devices

Angelika Peer and Martin Buss

Institute of Automatic Control Engineering, Technische Universität München, Germany
(Tel : +49-89-289-23412; E-mail: Angelika.Peer@tum.de, mb@tum.de)

Abstract: One of the main challenges in telerobotics is the selection of control architectures and control parameters, which are able to robustly stabilize the overall teleoperation system despite of changing human operator and environment impedances. In this paper robust stability of different types of bilateral control algorithms for admittance type devices is analyzed. Hereby, stability of the system is investigated by using the parameter space approach, which allows the analysis of uncertain systems with varying plant parameters. Simple linear models are assumed for human operator, human-system interface, teleoperator as well as remote environment. The parameter space method is used for controller design, as well as for robustness analysis. Finally, Γ -stability of the presented architectures is evaluated for a one degree-of-freedom mechatronic teleoperation system.

Keywords: bilateral teleoperation, robust stability, parameter space approach

1. INTRODUCTION

In a teleoperation system a human operator controls a remotely located teleoperator by a human-system interface. A typical bilateral teleoperation system is hereby formed by the main components human operator, human-system interface, communication channel, teleoperator, and environment. Master and slave devices are controlled by local controllers, which are coupled with each other over a communication channel. Since the human operator can behave in vary different ways and interact with different kind of remote environments ranging from free space to hard contact, one of the main challenges in telerobotics is the selection of robustly stable control architectures and corresponding control parameters. Typical approaches are either based on the passivity theorem [1], see e.g. [2–4], or the analysis of absolute stability by using Llewellyns stability criteria [5], see [6, 7] for examples. But the drawback of these approaches is that a passive human operator and remote environment have to be assumed. This work aims at analyzing stability by using the so called parameter space approach, which allows the analysis of uncertain systems with varying plant parameters. The parameter space method is used in a first step for controller design and in a second step for robustness analysis.

In the following section different types of bilateral control architectures for admittance-type devices are presented. Sec. 3 shows the principle of the parameter space approach and Sec. 4 introduces the models used for stability analysis. Finally in Sec. 5 robust stability of the presented control architectures is analyzed for a one degree of freedom mechatronic teleoperation system.

2. BILATERAL CONTROL ARCHITECTURES

Control architectures for bilateral teleoperation systems are commonly classified according to the number and kind of variables transmitted between master

and slave device, see [8] for an overview. So called two-channel control architectures, whereby master and slave are connected with each other via two communication channels, represent possibly the most popular bilateral controllers, see [9] for more details. Hereby, forces/positions are exchanged between master and slave device and local position or force controllers are used. While for impedance-type devices, which are characterized by very light-weight constructions with low inertia and friction, high performance force controllers can be implemented, for admittance-type devices, force control can only be realized with a very poor performance [10]. This is mainly due to the high dynamic properties and friction effects of admittance-type devices, which can only be compensated by using some kind of low level position controller. For further details on impedance and admittance-type devices see [11]. On this account classical bilateral control architectures with local force control are usually not very appropriate for teleoperation systems using admittance-type master and slave devices.

Commonly, admittance-type devices are controlled by using a so called position-based admittance control architecture, see [10]. Depending on the application, such an architecture can be either used to render a target dynamics or to achieve a certain compliant behavior when being in contact with the environment. In both cases the desired behavior is achieved by implementing impedances in form of simple mass-spring-damper systems

$$\mathbf{f} = \mathbf{M}\ddot{\mathbf{x}} + \mathbf{B}\dot{\mathbf{x}} + \mathbf{K}\mathbf{x}, \quad (1)$$

whereby \mathbf{x} are positions, \mathbf{f} are forces and \mathbf{M} means the mass, \mathbf{B} the damping and \mathbf{K} the stiffness matrix.

When rendering desired impedances, as shown in Fig. 1, the impedance is used to implement a desired target dynamics, e.g. the dynamics of a tool, which is attached to the end-effector. When trying to achieve a compliant behavior, as shown in Fig. 2, the impedance is used to modulate the desired position x_d , whereby the stiffness parameter defines an upper bound of displayable

stiffnesses. As shown below in both cases the impedance is lower bounded due to actuator limitations.

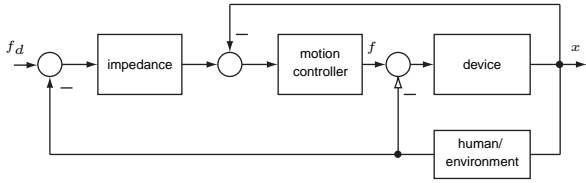


Fig. 1 Position-based admittance control used to render a target dynamics (Fa)

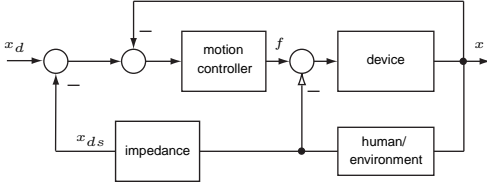


Fig. 2 Position-based admittance control used to achieve compliant behavior when being in contact (Pa)

In view of the classical two-channel control architectures, position-based admittance controllers can be implemented for master as well as slave devices and combined into a teleoperation control architecture when positions and forces are exchanged. Please observe that then ideal transparency cannot any more be achieved, since transparency is affected by the implemented desired master and slave impedances.

In principle three basic bilateral control architectures using local position-based admittance controllers can be realized:

2.1 Position-based admittance control with position-force exchange

In the position-based admittance control with position-force exchange, see Fig. 3, positions are sent from master to slave and forces from slave to master. Admittance type controllers are used to control master as well as slave device. The corresponding control laws are given by

$$f_m = D_{xm}(\dot{x}_{dm} - \dot{x}_m) + K_{xm}(x_{dm} - x_m), \quad (2)$$

$$f_s = D_{xs}(\dot{x}_d - \dot{x}_s) + K_{xs}(x_m - x_{ds} - x_s), \quad (3)$$

$$f_{ss} - f_{sm} = m_{dm}\ddot{x}_{dm} + b_{dm}\dot{x}_{dm}, \quad (4)$$

$$f_{ss} = m_{ds}\ddot{x}_{ds} + b_{ds}\dot{x}_{ds} + c_{ds}x_{ds} \quad (5)$$

for master and slave. While at master side a sort of force-control is implemented, at slave side a compliant controller is realized. During free space motion only the master impedance given by m_{dm} and b_{dm} is active, the slave side is controlled by a pure position controller. In contact also the slave impedance is active and both controllers influence the impression of the remote environment. In particular it should be noted that the stiffness parameter c_{ds} defines a lower bound of displayable stiffnesses.

2.2 Position-based admittance control with force-position exchange

The position-based admittance control with force-position exchange represents the mirrored version of the

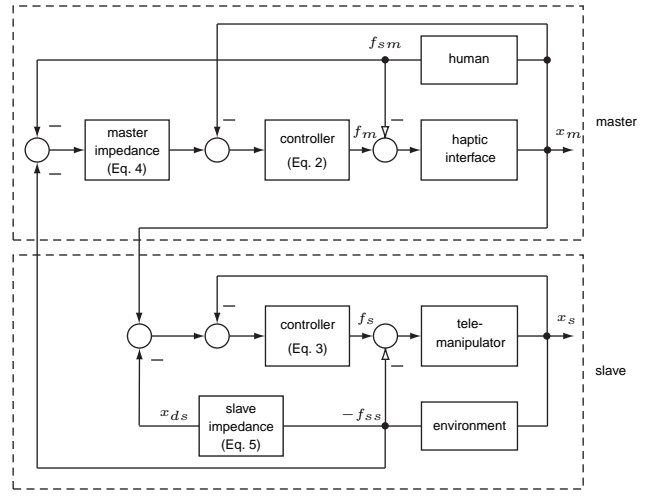


Fig. 3 Position-based admittance control with position-force exchange

last presented control architecture: forces are sent from master to slave and positions from slave to master. The corresponding control laws are given by

$$f_m = D_{xm}(\dot{x}_s - \dot{x}_{dm} - \dot{x}_m) + K_{xm}(x_s - x_{dm} - x_m), \quad (6)$$

$$f_s = D_{xs}(\dot{x}_{ds} - \dot{x}_s) + K_{xs}(x_{ds} - x_s), \quad (7)$$

$$-f_{sm} = m_{dm}\ddot{x}_{dm} + b_{dm}\dot{x}_{dm} + c_{dm}x_{dm}, \quad (8)$$

$$f_{ss} - f_{sm} = m_{ds}\ddot{x}_{ds} + b_{ds}\dot{x}_{ds}. \quad (9)$$

2.3 Position-based admittance control with force-force exchange

Finally, the position-based admittance control with force-force exchange, see Fig. 4, is characterized by a bilateral force-force exchange between master and slave. At both sides an admittance control strategy is implemented:

$$f_m = D_{xm}(\dot{x}_{dm} - \dot{x}_m) + K_{xm}(x_{dm} - x_m), \quad (10)$$

$$f_s = D_{xs}(\dot{x}_{ds} - \dot{x}_s) + K_{xs}(x_{ds} - x_s), \quad (11)$$

$$f_{ss} - f_{sm} = m_d\ddot{x}_{dm} + b_d\dot{x}_{dm}, \quad (12)$$

$$f_{ss} - f_{sm} = m_d\ddot{x}_{ds} + b_d\dot{x}_{ds}. \quad (13)$$

In order to guarantee position tracking the same impedances given by the mass m_d and the damping b_d have to be implemented for master and slave. On this account only two control parameters have to be selected, which simplifies tuning of the controller significantly.

3. PARAMETER SPACE APPROACH

Since in telemanipulation systems the operator interacts with environments of different impedances, we have to deal with an uncertain plant defined by the operating domain Q :

$$Q = \{q \mid q_i \in [q_i^-, q_i^+], i = 1, 2, \dots, l\}. \quad (14)$$

Thus, the stability analysis is performed by applying the parameter space approach [12], which allows the analysis of uncertain systems with varying plant parameters. It is

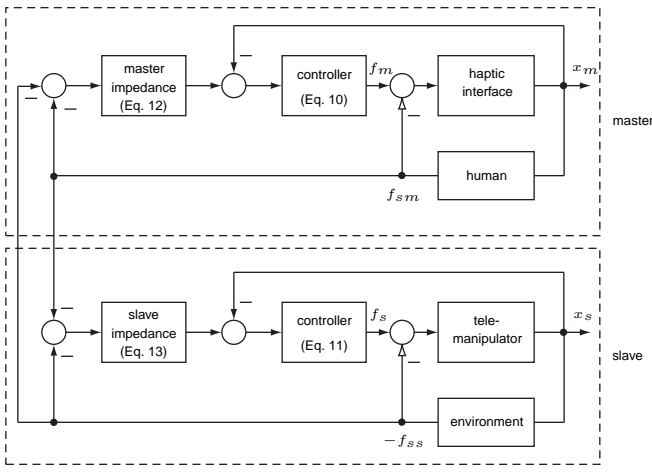


Fig. 4 Position-based admittance control with force-force exchange

based on the boundary crossing theorem of polynomials stated by Frazer and Duncan. Given the linear state space model

$$\dot{x} = Ax + Bu, \quad (15)$$

$$y = Cx + Du, \quad (16)$$

and the corresponding characteristic polynomial

$$p(s, \mathbf{q}) = \det(s\mathbf{E} - \mathbf{A}) = 0, \quad (17)$$

stability can be analyzed as follows:

The parameter space approach allows mapping of stability regions (further on referred as Γ -region) defined in the s -plane

$$\delta\Gamma := \{s \mid s = \sigma(\alpha) + j\omega(\alpha), \alpha \in [\alpha^-, \alpha^+]\} \quad (18)$$

into the parameter space formed by l uncertain plant or control parameters collected in the parameter vector \mathbf{q} . Hereby α means a generalized frequency. According to the boundary crossing theorem, starting from a stable characteristic polynomial $p(s, \mathbf{q})$, a polynomial with real coefficients $a_i(\mathbf{q})$ can only become unstable if the system crosses the stability boundary. Depending on whether the stability boundary is crossed on the real axis, imaginary axis or at infinity, real root boundaries (RRB), complex root boundaries (CRB) and infinite root boundaries (IRB) are distinguished. These boundaries are mapped into the parameter space by solving the following equations for the uncertain parameters $q_i = f(\alpha)$:

$$\begin{aligned} \text{RRB: } & p(\sigma_0, \mathbf{q}) = 0 \quad \text{with } \sigma_0 \text{ the} \\ & \text{intersection point of the real axis with } \delta\Gamma, \\ \text{IRB: } & \lim_{\alpha \rightarrow \infty} p(\sigma(\alpha) + j\omega(\alpha), \mathbf{q}) = 0, \\ \text{CRB: } & \Gamma_{CRB} := \{\mathbf{q} \mid p(\sigma(\alpha) + j\omega(\alpha), \mathbf{q}) = 0, \\ & p(\sigma + j\omega) \in \delta\Gamma, \alpha \in [\alpha^-, \alpha^+]\} \end{aligned} \quad (19)$$

The parameter space method can be either used for controller design or for robustness analysis, depending on whether the stability region is mapped into the parameter space of control parameters or varying plant parameters.

Controller design: The stability boundaries are mapped into a plane formed by two control parameters

k_1, k_2 . This allows to determine the set of control parameters for which the system is Γ -stable. If a system with n control parameters is considered, $n - 2$ control parameters must be fixed to a certain value, while the rest can be gridded. For each grid point the Γ -stability boundaries are computed and projected into the selected parameter plane.

Designing a controller for an uncertain plant requires basically two steps: In the first step sets of stabilizing controllers for some representative operating points (typically the vertices of the operating domain) have to be computed. The intersection of all these sets guarantees Γ -stability for all representative operating points, but not necessarily for the whole operating domain. After selection of appropriate control parameters this has to be verified in the second step by a robustness analysis.

Robustness analysis: The stability boundaries are mapped into a plane formed by two varying plant parameters q_1, q_2 . The system is robustly Γ -stable if the entire operating domain is contained in the Γ -stable parameter set.

4. MODELLING OF TELEOPERATION SYSTEM

To analyze stability of the teleoperation system a state space model of the overall system including haptic interface, telemanipulator, human and environment is needed. In the context of this work simple one degree of freedom models for haptic interface and telemanipulator are used. The human operator and the environment are modelled by using linear mass-spring-damper models. In the following these models are described in more detail.

4.1 Haptic interface and human operator

A very simple way to model a haptic interface is to use a mass-damper system [3] as shown in Fig. 5. Hereby m_m means the haptic interface mass and b_m the damping coefficient. The actuator force is modelled by f_m .

Since the human operator interacts with the haptic interface also a simple model of the human arm is needed. According to [13] a simple mass-spring-damper model can be used. In this context m_h means the human arm mass, c_h the human arm stiffness and b_h the human arm damping. The factor $\alpha \in [0, 1]$ is used to take into account variable human arm impedances. The exogenous force applied by the human operator is modelled by f_h . Finally, m_{em} means the end-effector mass and f_{sm} the force measured by the force-torque sensor located at the tip of the haptic interface.

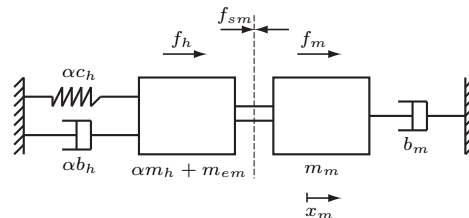


Fig. 5 Model of human system interface and human operator

The overall system described in Fig. 5 is represented by the following differential equations:

$$\begin{aligned} 0 &= f_h + f_{sm} - (\alpha m_h + m_{em}) \ddot{x}_m \\ &\quad - \alpha b_h \dot{x}_m - \alpha c_h x_m, \\ 0 &= f_{sm} - f_m + m_m \ddot{x}_m + b_m \dot{x}_m. \end{aligned} \quad (20)$$

4.2 Telemanipulator and environment

The telemanipulator is modelled analogously, whereby m_s means the telemanipulator mass, b_s the telemanipulator damping, and f_s the force applied by the actuators. The environment the telemanipulator interacts with is modelled by a mass-spring damper model. The end-effector mass and load is modelled by m_{es} , k_e and b_e mean the environmental stiffness and damping coefficient. The overall system is shown in Fig. 6 and can be described by using the following differential equations:

$$\begin{aligned} 0 &= f_s + f_{ss} - m_s \ddot{x}_s - b_s \dot{x}_s, \\ 0 &= f_{ss} + m_{es} \ddot{x}_s + b_e \dot{x}_s + c_e x_s. \end{aligned} \quad (21)$$

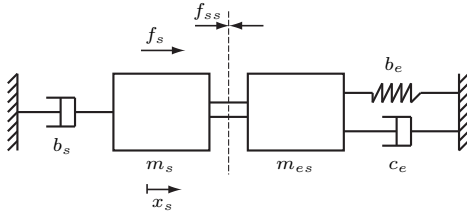


Fig. 6 Model of telemanipulator and environment

4.3 Actuator and sensor dynamics

In order to reproduce effects visible in the real hardware experiment also non-ideal actuator and sensor dynamics must be considered. On this account, the electrical motor time constant T_m is modelled by a low pass filter. Since measurements of the force-torque sensor are typically very noisy, they have to be filtered appropriately. Thus, also a simple low-pass filter with time constant T_f is considered.

5. STABILITY ANALYSIS FOR A ONE D.O.F TELEOPERATION SYSTEM

In this section stability of the above presented control algorithms for bilateral teleoperation is analyzed by using the parameter space approach. Hereby, in a first step sets of control parameters which stabilize the overall teleoperation system are determined and then a robustness analysis is carried out for one special set of control parameters.

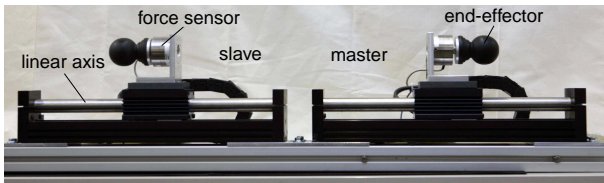


Fig. 7 Linear one d.o.f. teleoperation system

The numerical stability analysis is carried out for a linear one degree-of-freedom teleoperation system as shown

in Fig. 7. The teleoperation system consists of two identical linear axis (Thrusttube module) of Copley Controls Corp., which are used as master as well as slave devices. To measure the interaction force each device is additionally equipped with a one-degree-of-freedom force sensor (Burster, Model 2524). Position is measured by an optical encoder. The model parameters used for simulation are reported in Table 1. Hereby, the mass of each carriage and end-effector is measured, the damping coefficient is determined by system identification and the motor time-constant is taken from the technical data sheet. The force filter constant is selected to provide a good signal to noise ratio. Finally, in order to reduce the number of control parameters, the low level position controllers are assumed to be already tuned.

Table 1 Simulation parameters of one d.o.f. teleoperation system

parameter	value	parameter	value
m_m	2.386 kg	T_f	0.0032 s
b_m	20 Ns/m	T_m	0.00065 s
m_{em}	0.112 kg	K_{xm}	70,000
m_s	2.386 kg	D_{xm}	530
b_s	20 Ns/m	K_{xs}	70,000
m_{es}	0.112 kg	D_{xs}	530

All simulations were carried out for a three-dimensional operating domain formed by the varying parameters: environment stiffness $c_e \in [0 \ 10,000]$ N/m, environment damping $b_e \in [0 \ 200]$ Ns/m, and load mass $m_{es} \in [m_{es}^{min} \ m_{es}^{min} + 1]$ kg. This assumption is made because in a teleoperation system the operator can interact with different kind of environments, ranging from free space to hard contact. In addition, the operator can grasp objects, which has to be considered in the model. On this account, a varying load mass m_{es} is introduced, whereby the lower bound is given by the end-effector mass only.

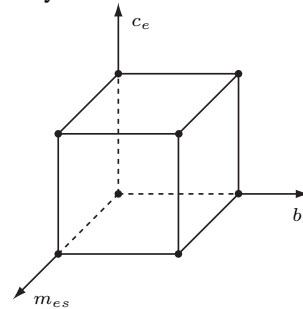


Fig. 8 Operating domain formed by environment stiffness, environment damping, and end-effector mass (including load mass)

In the following results of the numerical stability analysis for the above presented bilateral teleoperation control schemes are reported.

5.1 Position-based admittance control with position-force exchange (FaPa)

Using the position-based admittance control with position-force exchange five control parameters m_{dm} ,

b_{dm} , m_{ds} , b_{ds} , and c_{ds} have to be selected to guarantee stability of the overall teleoperation system. Hereby m_{dm} , b_{dm} mostly affect the free space behavior and m_{ds} , b_{ds} , c_{ds} the impression of contact. Further it is known that due to the admittance-type control the minimum target inertia of the master device is bounded by stability. On this account, m_{dm} has been set to a value which stabilizes the haptic interface, when used in standalone mode. In order to further reduce the number of control parameters $c_{ds}=1,000$ N/m has been fixed. It should be noted that the stiffness parameter c_{ds} mainly influences the perception of stiff environments since it introduces a upper bound for displayable stiffnesses. Thus, it should be selected carefully.

In the first step Hurwitz stability is analyzed. Fig. 9 shows the resulting stability boundaries which are mapped into the m_{ds} , b_{ds} plane, whereby b_{dm} is gridded. Each of the lines represent a set of stability margins determined for one of the eight vertices of the operating domain. The intersection of all these sets describes control parameters which stabilize all representative points. It can be seen that an increasing damping factor at master side increases the set of stabilizing controllers. Fig. 10 shows the dependency on the human arm impedance, whereby lowering the impedance significantly reduces the set of stabilizing controllers. Summarizing, it can be stated that in order to stabilize the system a low value for m_{ds} and a certain amount of b_{ds} is needed. Increasing the damping at operator side increases the set of stabilizing controllers, but reduces also significantly the free-space impression.

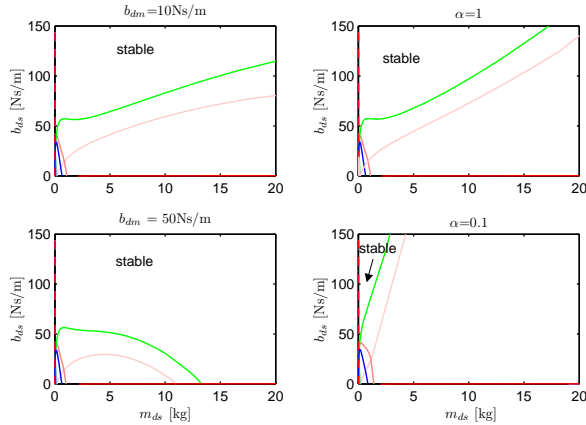


Fig. 9 FaPa architecture: Stability boundaries of the vertices of the operating domain in the (m_{ds}, b_{ds}) -plane depending on the damping parameter b_{dm} ($\alpha = 1$, $m_{dm} = 3$ kg, $c_{ds} = 1,000$ N/m).

Fig. 10 FaPa architecture: Stability boundaries of the vertices of the operating domain in the (m_{ds}, b_{ds}) -plane depending on the human arm impedance ($m_{dm} = 3$ kg, $b_{dm} = 0$ Ns/m, $c_{ds} = 1,000$ N/m).

Finally Fig. 11 serves as robustness analysis. Selecting one special controller out of the set of stabilizing controllers allows to robustly Γ -stabilize the telemanipulation

system since the entire operating domain is enclosed by the Γ -stability margins. When selecting a controller the smallest possible desired impedances should be chosen since these parameters directly affect the impression of the remote environment and reduce transparency of the overall teleoperation system. Further it should be noted that due to actuator limitations there is also a lower bound on the slave mass that can be implemented without causing instability of the teleoperator.

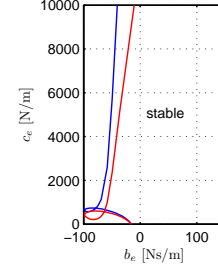


Fig. 11 Robustness analysis for FaPa-architecture: Stability boundaries of the vertices of the operating domain in the (b_e, c_e) -plane ($b_{ds} = 70$ Ns/m, $\alpha = 1$, $b_{dm} = 10$ Ns/m, $m_{dm} = 3$ kg, $m_{ds} = 1$ kg, $c_{ds} = 1,000$ N/m).

After implementing this control algorithm in the real hardware setup a relatively low damped behavior could be observed, when touching stiff environments. On this account, the analysis presented before has been carried out again for a new Γ -region as shown in Fig. 16. This new Γ -region guarantees a certain damping $D = -\sigma_i/\omega_0$ of the overall system. Fig. 12 shows the result of the corresponding stability analysis. Although a relatively small damping coefficient has been selected, the set of stabilizing controllers is reduced significantly. Increasing the damping coefficient even further would cause a dramatical reduction of stabilizing controller sets. This again indicates that a high slave damping has to be implemented in order to guarantee a good damped behavior, otherwise the interaction with stiff environments would inevitably cause oscillations.

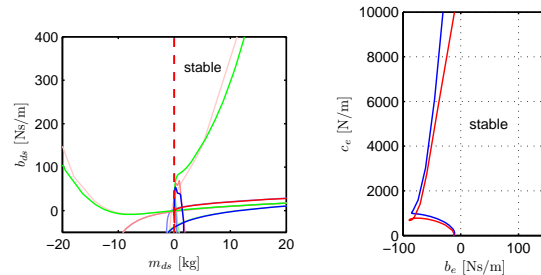


Fig. 12 FaPa architecture: Stability boundaries of the vertices of the operating domain in the (m_{ds}, b_{ds}) -plane and robustness analysis in the (b_e, c_e) -plane for a damping of $D = -0.1$ ($\alpha = 1$, $m_{dm} = 3$ kg, $b_{dm} = 10$ Ns/m, $m_{ds} = 1$ kg, $b_{ds} = 100$ Ns/m, $c_{ds} = 1,000$ N/m).

5.2 Position-based admittance control with force-position exchange (PaFa)

Again five control parameters m_{dm} , b_{dm} , c_{dm} , m_{ds} , b_{ds} have to be selected in order to guarantee Γ -stabilizing behavior. The same principle as presented above is used to reduce the number of variable control parameters: m_{ds} is selected to stabilize the telemanipulator alone and c_{dm} is fixed.

The results gained from the parameter space approach are shown in Fig. 13. The bigger the slave damping b_{ds} , the larger is the set of stabilizing control parameters. Fig.14 shows the stability margins dependent on the human arm impedance. If the slave damping is selected high enough an increasing human arm impedance decreases the set of stabilizing controllers. Finally Fig. 15 serves as robustness analysis.

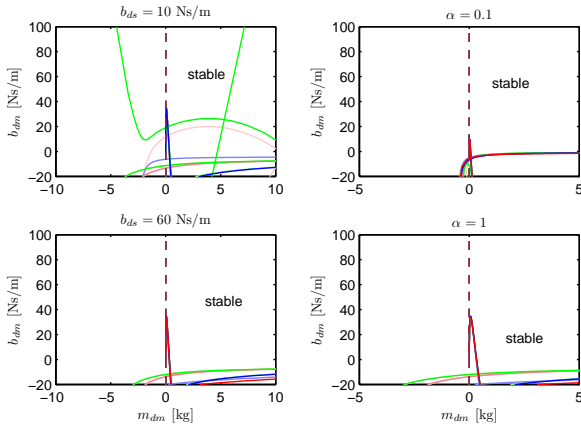


Fig. 13 PaFa architecture: Stability boundaries of the vertices of the operating domain in the (m_{dm}, b_{dm}) -plane depending on the damping parameter b_{ds} ($\alpha = 1$, $m_{ds} = 3$ kg, $c_{dm} = 1,000$ N/m).

Fig. 14 PaFa architecture: Stability boundaries of the vertices of the operating domain in the (m_{dm}, b_{dm}) -plane depending on the human arm impedance ($m_{ds} = 3$ kg, $b_{ds} = 60$ Ns/m, $c_{dm} = 1,000$ N/m).

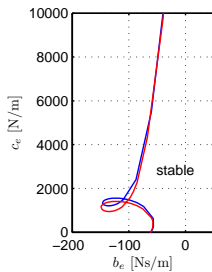


Fig. 15 Robustness analysis for PaFa-architecture: Stability boundaries of the vertices of the operating domain in the (b_e, c_e) -plane ($b_{ds} = 60$ Ns/m, $m_{ds} = 3$ kg, $m_{dm} = 1$ kg, $b_{dm} = 30$ Ns/m, $c_{dm} = 1,000$ N/m, $\alpha = 1$).

In order to be able to manipulate objects and to interact with different kind of impedances, a damped behavior of

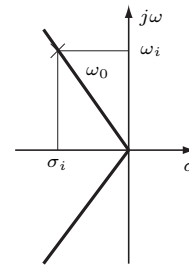


Fig. 16 Γ -region with damping $D = -\sigma_i/\omega_i$

the overall system is necessary. The influence of the required damping on the control parameters is analyzed in Fig. 17. Again a Γ -region with damping $D = -0.1$ is selected and the stability margins are plotted. The analysis shows that the region of stabilizing controllers is reduced. Especially for high human arm impedances the overall system can only be stabilized if small values for the master mass m_{dm} and a certain amount of damping b_{dm} are selected. Otherwise Γ -stability cannot be guaranteed.

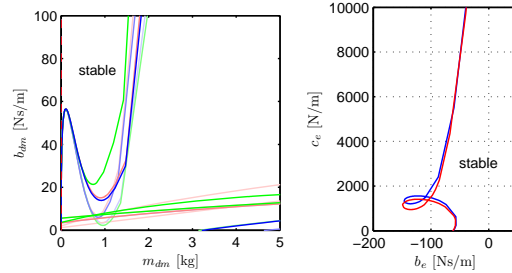


Fig. 17 PaFa architecture: Stability boundaries of the vertices of the operating domain in the (m_{dm}, b_{dm}) -plane and robustness analysis in the (b_e, c_e) -plane for a damping of $D = -0.1$ ($\alpha = 1$, $m_{dm} = 1$ kg, $b_{dm} = 50$ Ns/m, $m_{ds} = 3$ kg, $b_{ds} = 60$ Ns/m, $c_{dm} = 1,000$ N/m).

5.3 Position-based admittance control with force-force exchange (FaFa)

Using a position-based admittance control with force-force exchange, position tracking can only be guaranteed if equal desired impedances are selected at master as well as slave side. Thus, the number of control parameters can be reduced to a minimum of two variable parameters m_d , b_d . The characteristic polynomial of this setup is characterized by a bilinear dependency of the two uncertain control parameters in the polynomial coefficients. On this account, the mapping of the stability boundaries into the parameter space of the control parameters m_d , b_d causes some difficulties. To overcome these problems the parameters m_d , b_d are gridded and the poles of the corresponding characteristic polynomial are computed. The stability boundary can then be determined by using a bisection algorithm, which tries to find for a fixed m_d the value b_d that lies on the stability boundary. This procedure is repeated for every vertex of the operating domain.

The result is shown in Fig. 18. Selecting a desired mass m_d in general a certain amount of damping b_d is necessary to Γ -stabilize the system. There exists only a

very small area, where a desired mass m_d stabilizes the system without implementing additional damping. The parameter m_d should be selected at least that large that haptic interface and telemanipulator are stable when they are operated alone. Finally, Fig. 18 right shows the stability boundaries in the b_e, c_e -plane. Since the polynomial depends affine on the parameters b_e, c_e the parameter space approach is used again. It can be seen that the selected control parameters stabilize the overall operating domain. Finally, selecting a Γ -region with damping $D = -0.1$ a certain amount of damping is necessary to Γ -stabilize the system when being in contact with stiff remote environments, see Fig. 19.

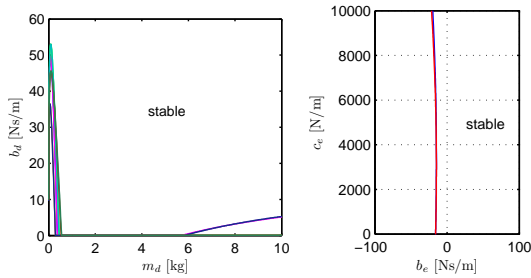


Fig. 18 FaFa architecture: Stability boundaries of the vertices of the operating domain in the (m_d, b_d) -plane and robustness analysis in the (b_e, c_e) -plane ($\alpha = 1, b_d = 10$ Ns/m, $m_d = 3$ kg).

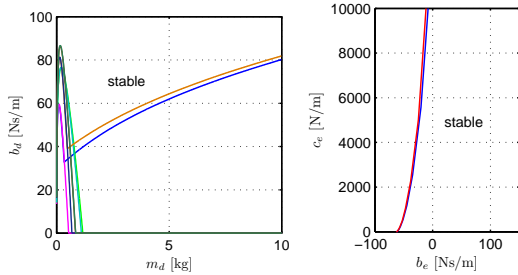


Fig. 19 FaFa architecture (linear one d.o.f. device): Stability boundaries of the vertices of the operating domain in the (m_d, b_d) -plane and robustness analysis in the (b_e, c_e) -plane for a damping of $D = -0.1$ ($\alpha = 1, m_d = 3$ kg, $b_d = 60$ Ns/m).

6. SUMMARY AND CONCLUSION

A stability analysis of different types of bilateral control architectures using admittance-type devices has been carried out. Robust stability has been investigated by using the parameter space approach, which allows the analysis of uncertain systems with varying plant parameters. In contrast to other approaches known from literature no passive human operator as well as remote environment have to be assumed. For the analysis simple linear models for haptic interface and teleoperator have been taken. Moreover varying impedance models have been used for human operator and remote environment and the actuator dynamics has been considered. Finally, the approach has been applied to a one d.o.f. teleoperation system and robustly stabilizing controllers have been determined for each of the before presented teleoperation architectures.

ACKNOWLEDGMENTS

This work is supported in part by the German Research Foundation (DFG) within the collaborative research center SFB453 "High-Fidelity Telepresence and Teleaction".

REFERENCES

- [1] G. Raisbeck, "A Definition of Passive Linear Networks in Terms of Time and Energy," *Journal of Applied Physics*, vol. 25, pp. 1510–1514, 1954.
- [2] D. Lawrence, "Stability and Transparency in Bilateral Teleoperation," *IEEE Trans. on Robotics and Automation*, vol. 9, no. 5, pp. 624–637, 1993.
- [3] Y. Yokokohji and T. Yoshikawa, "Bilateral Control of Master-Slave Manipulators for Ideal Kinesthetic Coupling-Formulation and Experiment," *IEEE Trans. on Robotics and Automation*, vol. 10, no. 5, pp. 605 – 620, 1994.
- [4] D. Lee and M. Spong, "Passive Bilateral Teleoperation With Constant Time Delay," *IEEE Trans. on Robotics and Automation*, vol. 22, no. 2, pp. 269–281, 2006.
- [5] F. Llewellyn, "Some Fundamental Properties of Transmission Systems," in *Proc. of the IRE*, vol. 40, March 1952, pp. 271–283.
- [6] R. J. Adams and B. Hannaford, "Stable Haptic Interaction with Virtual Environments," *IEEE Trans. on Robotics and Automation*, vol. 14, no. 3, pp. 465–474, 1999.
- [7] K. Hashtrudi-Zaad and S. E. Salcudean, "Analysis of Control Architectures for Teleoperation Systems with Impedance/Admittance Master and Slave Devices," *The International Journal of Robotics Research*, vol. 20, no. 6, pp. 419–445, June 2001.
- [8] S. Hirche, M. Ferre, J. Barrio, C. Melchiorri, and M. Buss, "Bilateral Control Architectures for Telerobotics," in *Advances in Telerobotics*, M. Ferre, M. Buss, R. Aracil, C. Melchiorri, and C. Balaguer, Eds. Berlin: Springer STAR series, 2007.
- [9] J. Kim, P. Chang, and H. Park, "Transparent Teleoperation Using Two-Channel Control Architectures," in *Proc. of the IEEE/RSJ International Conference on Robots and Systems*, 2005, pp. 2824–2831.
- [10] M. Ueberle and M. Buss, "Control of Kinesthetic Haptic Interfaces," in *Proc. of the IEEE/RSJ International Conference on Intelligent Robots and Systems, Workshop on Touch and Haptics*, 2004.
- [11] C. Clover, G. Luecke, J. Troy, and W. McNeely, "Dynamic Simulation of Virtual Mechanisms With Haptic Feedback Using Industrial Robotics Equipment," in *Proc. of the IEEE International Conference on Robotics and Automation*, 1997, pp. 724–730.
- [12] J. Ackermann, *Robust Control, The Parameter Space Approach*, 2nd ed. London: Springer, 2002.
- [13] D. Lawrence and J. Chapel, "Performance Trade-Offs for Hand Controller Design," in *Proc. of the IEEE International Conference on Robotics and Automation*, 1994, pp. 3211–3216.